

PAPER • OPEN ACCESS

## Microstructure and magnetic properties of $\text{Co}_{58}\text{Ni}_{10}\text{Fe}_5\text{B}_{16}\text{Si}_{11}$ and $\text{Co}_{58}\text{Ni}_{10}\text{Fe}_5\text{B}_{16}\text{Si}_{11}\text{-Al}_2\text{O}_3$ bulk amorphous coatings prepared by plasma spraying

To cite this article: E A Denisova *et al* 2020 *J. Phys.: Conf. Ser.* **1582** 012078

View the [article online](#) for updates and enhancements.



**IOP | ebooks™**

Bringing together innovative digital publishing with leading authors from the global scientific community.

Start exploring the collection—download the first chapter of every title for free.

# Microstructure and magnetic properties of $\text{Co}_{58}\text{Ni}_{10}\text{Fe}_5\text{B}_{16}\text{Si}_{11}$ and $\text{Co}_{58}\text{Ni}_{10}\text{Fe}_5\text{B}_{16}\text{Si}_{11}\text{-Al}_2\text{O}_3$ bulk amorphous coatings prepared by plasma spraying

E A Denisova<sup>1,2</sup>, I V Nemtsev<sup>3</sup>, S V Telegin<sup>4</sup>, R S Iskhakov<sup>1</sup>, L A Kuzovnikova<sup>5</sup>,  
N A Shepeta<sup>2,4</sup>

<sup>1</sup>Kirensky Institute of Physics, SB Russian Academy of Sciences, 50/38, Akademgorodok str., Krasnoyarsk, 660036, Russia

<sup>2</sup>Siberian Federal University, 79, Svobodny ave., Krasnoyarsk, 660041, Russia

<sup>3</sup>Scientific Center, Federal Research Center KSC SB RAS, 50, Akademgorodok str., Krasnoyarsk, 660036, Russia

<sup>4</sup>Reshetnev Siberian State University of Science and Technology, 31, Krasnoyarsky Rabochy ave., 660037, Krasnoyarsk, Russia

<sup>5</sup>Krasnoyarsk Institute of Railways Transport, 2И, Novaja Zarja str., Krasnoyarsk, Russia

E-mail: kuzovnikova\_la@krsk.irkups.ru

**Abstract.** The bulk soft magnetic glassy  $\text{Co}_{58}\text{Ni}_{10}\text{Fe}_5\text{B}_{16}\text{Si}_{11}$  alloy specimens have been prepared by plasma spray deposition. In order to increase resistivity of the material, the bulk  $\text{Co}_{58}\text{Ni}_{10}\text{Fe}_5\text{B}_{16}\text{Si}_{11}\text{-Al}_2\text{O}_3$  composite materials were fabricated. The investigations of structure and magnetic properties of the bulk samples were carried out by X-ray diffraction, electron microscopy and magnetic measurements. The relation of the structural features and magnetic characteristics of the bulk coating to the main parameters of the deposition regimes was determined. Optimized plasma spray deposition parameters allowed obtaining bulk glassy samples with magnetic parameters that are not inferior to the characteristics of a thermally treated rapidly quenched ribbon with the same composition. It was found that the bulk amorphous coatings can be characterized as a heterophase system. The relaxation annealing of the  $\text{Co}_{58}\text{Ni}_{10}\text{Fe}_5\text{B}_{16}\text{Si}_{11}$  bulk coating leads to a phase transition in this alloy in the precrystallization temperature range. The magnetic properties of the both kinds of coatings are correlated with changes in the microstructure. The appearance of nanocrystalline phase with  $T_c \sim 640$  K during relaxation heat treatment leads to a decrease of the coercivity and to an increase of the permeability. A comparison between the magnetic properties of the  $\text{CoNiFe-BSi}$  coating and  $(\text{CoNiFe-BSi})\text{-Al}_2\text{O}_3$ , composite coating is carried out.

## 1. Introduction

Fe- and Co-based bulk metallic glasses exhibit attractive combinations of chemical, mechanical, and magnetic properties [1-7]. They are suitable materials for many electrical devices such as electronic measuring and surveillance systems, magnetic sensors, magnetic shielding, precision mold material, and cutting tool material. The industrial application of these materials requires both their successful consolidation into bulk body and preservation of their structure. Nanostructured and amorphous



coatings without grain growth can be formed by a variety of methods [8-12], but the plasma spray process permits the use of complex geometry substrates.

Plasma spray processing is a droplet deposition method that combines the steps of melting, rapid solidification, and consolidation into a single step. In the last decade, bulk ferromagnetic Fe-based glassy alloys with good soft magnetic properties have been synthesized [13-14]. The preparation of composite materials consisting of nanocrystalline metallic layers separated by insulator layers, makes it possible to get rid of the eddy current frequency limit [15].

The primary requirements for a soft magnetic material include high initial permeability, high saturation magnetization, low coercivity, and low core loss. In such materials, the magnetization process is easiest and a narrow hysteresis loop results, leading to small energy losses under cyclic magnetization. It was found [16] that the desired magnetic properties of  $\text{Co}_{58}\text{Ni}_{10}\text{Fe}_5\text{B}_{16}\text{Si}_{11}$  bulk alloy (zero magnetostriction, high initial and maximum magnetic permeability, etc.) can be achieved by a formation of coating with a certain amorphous/crystalline phase ratio. This paper deals with progress in stabilization of amorphous or nanostructured state of bulk  $\text{Co}_{58}\text{Ni}_{10}\text{Fe}_5\text{B}_{16}\text{Si}_{11}$  alloy prepared by plasma spray deposition. In order to increase resistivity of the material the bulk  $\text{Co}_{58}\text{Ni}_{10}\text{Fe}_5\text{B}_{16}\text{Si}_{11}$ - $\text{Al}_2\text{O}_3$  composite material was prepared. We focused on empirical rules for the achievement of local atomic configurations, structure with certain amorphous/nanocrystalline phase ratio, soft magnetic properties.

## 2. Materials and methods

Ball milling of  $\text{Co}_{58}\text{Ni}_{10}\text{Fe}_5\text{B}_{16}\text{Si}_{11}$  ribbons and subsequent plasma spraying of the resulting powders were used to prepare bulk amorphous samples. The details of the plasma spray deposition process were reported elsewhere [17].

Amorphous  $\text{Co}_{58}\text{Ni}_{10}\text{Fe}_5\text{B}_{16}\text{Si}_{11}$  powders were blended with  $\text{Al}_2\text{O}_3$  fine powders at different concentrations. Such powder mixtures were used as feedback for plasma spraying. Powder was spread on an aluminum pipe cooled with water or heated up in the temperature range from 273 to 673 K using the plasma spray process. The thickness of applied coatings was 3 mm.

The regimes of plasma spray deposition were selected so that the structure and the basic magnetic characteristics (the diffraction pattern, heat and temperature of crystallization  $T_{\text{crys}} \sim 540$  °C, saturation magnetization calculated per  $\text{Co}_{58}\text{Ni}_{10}\text{Fe}_5\text{B}_{16}\text{Si}_{11}$  phase volume,  $M_0 \sim 620$  G, exchange stiffness constant,  $D \sim 117$  meV $\cdot$ A<sup>2</sup>) would remain unchanged. Afterwards these coatings were subjected to heat treatment at a temperature ranging between 373 and 1073 K, and for an interval of 0.5 to 3 hours in argon atmosphere. The morphology and the composition of the investigated materials were analyzed using a scanning electron microscope (S5500 Hitachi and an energy-dispersive spectrometer TM3000).

The surface of a metallographic specimen was prepared by grinding, polishing, and etching in a mixture of nitric acid, hydrochloric acid and alcohol. The structure of the bulk coatings was determined using a DRON-4 X-ray diffractometer operating with Cu  $K\alpha$  radiation. The magnetization was measured as a function of temperature, field orientation using a vibrating sample magnetometer and PPMS. The amorphous/crystalline phase ratio was estimated using the technique of magnetic phase analysis. The phases were identified on the basis of their Curie temperature  $T_C$  and saturation magnetization  $M_0$ .

## 3. Results and discussion

The SEM images of cobalt-based plasma spray coating and composite coating are presented at Figure 1. The as-deposited bulk coatings of 3 mm present a dense layered structure with low porosity (1.9%), without cracking and with good adherence (figure 1a). EDX analysis shows that  $\text{Co}_{58}\text{Ni}_{10}\text{Fe}_5\text{B}_{16}\text{Si}_{11}$  coating with  $T_s < 200$  °C was characterized by homogeneous distribution of the elements (Figure 1b). In figure 1c you can see the image of  $\text{Co}_{58}\text{Ni}_{10}\text{Fe}_5\text{B}_{16}\text{Si}_{11}$ - $\text{Al}_2\text{O}_3$  composite coating with 50%  $\text{Al}_2\text{O}_3$ . The picture demonstrates that the amorphous metallic particles percolate. The shiny areas correspond to metal grains. Figure 1d, e presents the corresponding Al and Co EDX

mapping of composite coating. You can see here that starting powder was consolidated without decomposition.

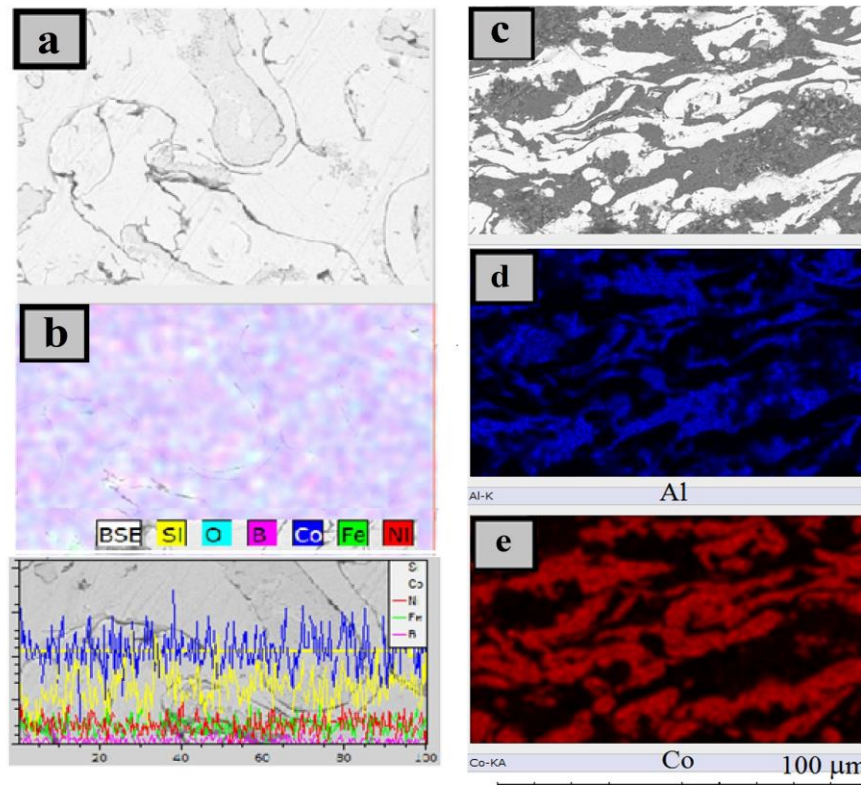


**Figure 1.** SEM images of bulk  $\text{Co}_{58}\text{Ni}_{10}\text{Fe}_5\text{B}_{16}\text{Si}_{11}$  coating (cross-section) (a) and EDX map (b); SEM images of bulk  $\text{Co}_{58}\text{Ni}_{10}\text{Fe}_5\text{B}_{16}\text{Si}_{11}\text{-Al}_2\text{O}_3$  composite coating with 50%  $\text{Al}_2\text{O}_3$  (c) and the corresponding Al (d) and Co (e) EDX mapping (f).

The XRD analysis revealed that the amorphous structure of  $\text{Co}_{58}\text{Ni}_{10}\text{Fe}_5\text{B}_{16}\text{Si}_{11}$  powders was preserved after plasma spray with the power of the electric arc levels  $P_a$  up to 20 kW and the substrate temperature  $T_s$  varying from 20 °C to 300 °C. In Figure 2 the XRD patterns of the  $\text{CoNiFe-BSi}$  bulk coating and  $\text{Co}_{58}\text{Ni}_{10}\text{Fe}_5\text{B}_{16}\text{Si}_{11}\text{-Al}_2\text{O}_3$  composite coating are plotted. The XRD pattern for the  $\text{CoNiFe-BSi}$  bulk coating consists only of halo. No appreciable diffraction peaks corresponding to a crystalline phase can be detected. Therefore, bulk coating consists of a glassy phase. For the composite coating case, the XRD peaks corresponding to the  $\text{Al}_2\text{O}_3$  phase and an amorphous halo corresponding to metal phase are presented together. A slight increase in the grain size from 8 nm to 14 nm, as determined from X-ray line widening measurements, was observed for both types of bulk coating.

In case of amorphous samples, the technique of magnetic phase analysis can provide additional information about material microstructure. Thermomagnetic curves for the  $\text{Co}_{58}\text{Ni}_{10}\text{Fe}_5\text{B}_{16}\text{Si}_{11}$  ribbon and coating,  $\text{Co}_{58}\text{Ni}_{10}\text{Fe}_5\text{B}_{16}\text{Si}_{11}\text{-Al}_2\text{O}_3$  composite coating are presented in Figure 3.

The results of thermomagnetic analysis of both type coating indicate that the initial alloy can be characterized as a heterophase system in which phase 1 with  $T_C \sim 550$  K comprises 90% of the volume for  $\text{Co}_{58}\text{Ni}_{10}\text{Fe}_5\text{B}_{16}\text{Si}_{11}$  coating and 80% of the volume for composite coating and the phase 2 with  $T_C \sim 840$  K comprises 10% and 20% respectively. The Curie temperatures of these phases are different and consequently chemical short-range order in these amorphous phases is different. Similar formation of several amorphous phases was also observed in [18].

It is found that the appearance of dispersed inclusions of phase 2 in phase 1 was stimulated by an increase of substrate temperature. In the case of composite coating, addition of  $\text{Al}_2\text{O}_3$  particles changes the heat transfer behavior and decrease the quenching rate, therefore  $\text{Co}_{58}\text{Ni}_{10}\text{Fe}_5\text{B}_{16}\text{Si}_{11}\text{-Al}_2\text{O}_3$  coating

contains a larger amount of the phase 2. In the case of  $\text{Co}_{58}\text{Ni}_{10}\text{Fe}_5\text{B}_{16}\text{Si}_{11}$  ribbon only one  $T_C \sim 510$  K was registered. The relaxation annealing of the both type bulk coating leads to a phase transition in this alloy in the precrystallization temperature range. At  $T_{an} \sim 300^\circ\text{C}$  the nanocrystalline phase inclusions with  $T_C \sim 600$  K arise. It can be noticed that as  $T_{an}$  increases the volume fraction of phase 1 ( $W_1$ ) decreases and  $W_2$  (phase 2) increases so that in the region  $400 < T_{an} < 450^\circ\text{C}$   $W_1 \approx W_2$ , and when  $T_{an} = 500^\circ\text{C}$   $W_2$  is much larger than  $W_1$ .

The best value of permeability  $\mu \sim 20 \cdot 10^3$  for CoNiFe-BSi coating is achieved when volume fraction of the phase 1 with  $T_C \sim 550$  K is decreased to 50% and nanocrystalline phase with  $T_C \sim 600$  K volume fraction is increased to 30%. So the optimized plasma spray deposition parameters (plasma current  $\sim 220\text{A}$ ,  $T_s < 150^\circ\text{C}$ ,  $P_a \sim 20$  kW) allowed to obtain bulk glassy samples with magnetic parameters that are not inferior to the characteristics of a thermally treated rapidly quenched ribbon with the same composition.

The variation of magnetization with temperature of both type of bulk samples obeys Bloch's law  $M(T) = M_0(1 - BT^{-3/2})$ . Using this equation we determined the value of Bloch constant,  $B$ , and saturation magnetization,  $M_0$ . The  $B$  and  $M_0$  values barely changed during plasma spray process. The saturation magnetization,  $M_0$ , is equal to 620 G for the initial ribbon. It is found that value of  $M_0$  remains unchanged with increasing of  $T_{an}$  up to  $700^\circ\text{C}$ . The increase in  $D$  value with  $T_{an} > 400^\circ\text{C}$  indicates that the volume fraction of nanocrystalline phase increases. The analysis of the magnetic hysteresis loops curves (Figure 4) shows that plasma spraying does not cause a change of coercive field ( $H_c$ ) value (0.3 Oe) for  $\text{Co}_{58}\text{Ni}_{10}\text{Fe}_5\text{B}_{16}\text{Si}_{11}$  coating. The oxide addition increased the coercivity of  $\text{Co}_{58}\text{Ni}_{10}\text{Fe}_5\text{B}_{16}\text{Si}_{11}-\text{Al}_2\text{O}_3$  coating up to 0.5 Oe. In order to increase the resistivity of material we produced the  $\text{Co}_{58}\text{Ni}_{10}\text{Fe}_5\text{B}_{16}\text{Si}_{11}-\text{Al}_2\text{O}_3$  composite coating.

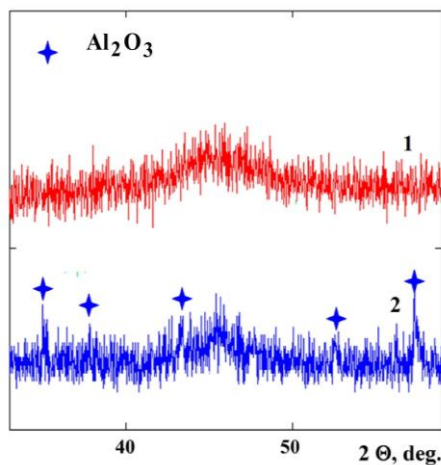


**Figure 2.** XRD patterns of the bulk CoNiFe-BSi coating (1) and (CoNiFe-BSi)- $\text{Al}_2\text{O}_3$  composite samples (2).

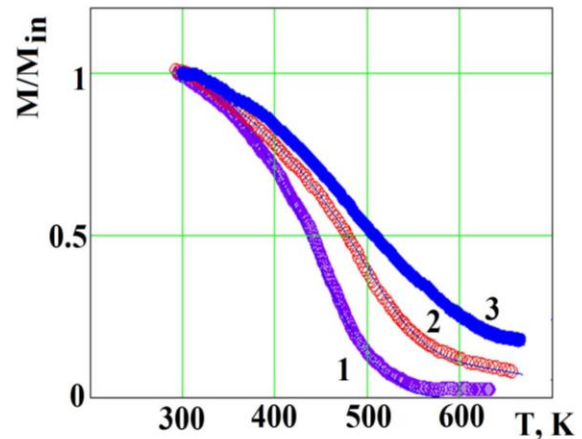


**Figure 3.** Thermomagnetic curves for the  $\text{Co}_{58}\text{Ni}_{10}\text{Fe}_5\text{B}_{16}\text{Si}_{11}$  initial ribbon (1), bulk amorphous coating (2) and composite coating (3).

**Table 1.** Magnetic characteristics of bulk coatings

	Saturation magnetization $M_0$ (G)	Stiffness constant $D$ ( $\text{meV} \cdot \text{Å}^2$ )	Permeability $\mu_{eff}$	Coercive field $H_c$ (Oe)	Electric resistivity $r$ ( $\mu\text{Ohm} \cdot \text{cm}^2$ )
Initial amorphous foil	620	117	$20 \cdot 10^3$	0,2	130
Coating CoNiFeBSi	620	117	$20 \cdot 10^3$	0,3	300
Composite CoNiFeBSi- $\text{Al}_2\text{O}_3$	620	117	$10 \cdot 10^3$	0,5	400-780

In this case the resistivity was increased up to 400-780  $\mu\text{Ohm}\cdot\text{cm}^2$  regardless of the  $\text{Al}_2\text{O}_3$  content. The frequency limit was shifted up to 1MHz. Table 1 summarizes magnetic properties of  $M_0$ ,  $\mu$  and  $H_c$  as well as electric resistivity of the glassy coating. The data of the ribbon are also shown for comparison.

#### 4. Conclusion

The bulk amorphous  $\text{Co}_{58}\text{Ni}_{10}\text{Fe}_5\text{B}_{16}\text{Si}_{11}$  alloys and  $\text{Co}_{58}\text{Ni}_{10}\text{Fe}_5\text{B}_{16}\text{Si}_{11}-\text{Al}_2\text{O}_3$  composite material were prepared by plasma spray deposition. Metallic glass and composite coatings formed on the aluminum substrate were of dense morphology with low porosity of 2% at plasma current of 220 A in about 3 mm thickness. The CoNiFe-BSi alloy for both types of coating consists of two amorphous magnetic phases: matrix of phase 1 with  $T_C \sim 550$  K and inclusion of the phase 2 with  $T_C \sim 840$  K. The volume of phase 2 becomes larger for higher substrate temperatures. It is found that the annealing of the  $\text{Co}_{58}\text{Ni}_{10}\text{Fe}_5\text{B}_{16}\text{Si}_{11}$  bulk coating in the precrystallization temperature range leads to a phase transition in this alloy. For plasma spraying CoNiFe-BSi coating the appearance of nanocrystalline phase with Curie temperature  $T_C \sim 640$  K during relaxation heat treatment and reducing of phase 1 volume up to 50% leads to a decrease of the coercivity (0.3 Oe) and to an increase of the permeability up to  $20 \cdot 10^3$ . The oxide addition increased the coercivity of  $\text{Co}_{58}\text{Ni}_{10}\text{Fe}_5\text{B}_{16}\text{Si}_{11}-\text{Al}_2\text{O}_3$  coating up to 0.5 Oe and the resistivity up to 400-780  $\mu\text{Ohm}\cdot\text{cm}^2$  regardless of the  $\text{Al}_2\text{O}_3$  content, and shifted frequency limit up to 1 MHz.

#### 5. Acknowledgments

This work was funded by the Russian Foundation for Basic Research, the Government of the Krasnoyarsk Territory, the Krasnoyarsk Regional Fund for the Support of Scientific and Technical Activities (project no. 18-42-240006 Nanomaterials with magnetic properties determined by the topological features of the nanostructure). The authors thank the Krasnoyarsk Regional Center of Research Equipment of Federal Research Center "Krasnoyarsk Science Center SB RAS" for the provided equipment.

#### References

- [1] Gleiter H 1989 *Prog. Mater. Sci.* **33** 223–315
- [2] Gleiter H 2000 *Acta Mater.* **48** 1–29
- [3] Inoue A 2001 *Mater. Sci. Eng. A* **304–306** 1–10
- [4] Wysłocki J J and Pawlik P 2010 *J. Achievements Mater. Manuf. Eng.* **43** 463–468
- [5] Ashish Singh, Srinivasa R Bakshi, Arvind Agarwal and Sandip P Harimkar 2010 *Materials Science and Engineering A* **527** 5000–5007
- [6] Shapaan M, Bárdos A, Lábár J, Lendvai J and Varga L K 2004 *Phys. status solidi* **201** 476–481
- [7] Inoue Akihisa and Takeuchi Akira 2004 *Materials Science and Engineering: A* **375–377** 16–30
- [8] Zhao Jian, Gao Qingwei, Wang Hougin, Shu Fengyuan, Zhao Hongyun, He Wenxiong and Yu Zhishui 2019 *Journal of Alloys and Compounds* **785** 846–854
- [9] Dong Qiangsheng, Zhang Baosen, Ba Zhixin, Li Zhuangzhuang and Wang Zhangzhong 2019 *Surf. Topogr.: Metrol. Prop.* **7** 044001
- [10] Lesz S, Babilas R, Nabiałek M, Szota M, Do'spiał M and Nowosielski R 2011 *Journal of Alloys and Compounds* **509S** S197–S201
- [11] Bitoh T, Makino A and Inoue A 2006 *J. Appl. Phys.* **99** 08F102
- [12] Fuzer J, Bednarcika J, Kollar P and Rothc S 2007 *Journal of Magnetism and Magnetic Materials* **316** e834–e837
- [13] Kobayashi Akira, Yano Shoji, Kimura Hisamichi and Inoue Akihisa 2008 *Materials Science and Engineering B* **148** 110–113
- [14] Yulong An, Guoliang Hou, Jie Chen, Xiaoqin Zhao, Guang Liu, Huidi Zhou and Jianmin Chen 2014 *Vacuum* **107** 132e140
- [15] Varga L K 2007 *J. Magn. Magn. Mater.* **316** 442–447

- [16] Lepeshev A A, Iskhakov R S, Denisova E A and Saunin V N 1995 *Tech. Phys. Lett.* **21** 641–643
- [17] Saunin V N, Telegin S V, Kalita V I and Denisova E A 2012 *Inorg. Mater. Appl. Res.* **3** 201–209
- [18] Abrosimova G E 2011 *Physics – Uspekhi. Advances in Physical Sciences* [in Russian – Uspekhi Fizicheskikh Nauk] **181** 1265-1281